International Journal for Multidisciplinary Research (IJFMR)
E-ISSN: 2582-2160 ● Website: www.ijfmr.com ● Email: editor@ijfmr.com

Investigation of Nuclear Structure and Characteristics of Select Intermediate N=88 Nuclei Using the IBM-2 Interacting Boson Model

Bashar. Hawi. Azeez Abu-Gebaz[1], Doaa katea ghali[2]

[1,2]Department of Physics, College of Science, AL-Muthanna University, AL-Muthanna, IRAQ

Abstract

The Hamiltonian model of the second interacting bosons was utilised to calculate the energy levels of the isotopes ${}^{144}_{88}Ba_{56}$,${}^{146}_{88}Ce_{58}$,${}^{148}_{88}Nd_{60}$. Upon calculating the ratio (E_{41}/E_{21}), it was determined that these isotopes are categorised within the O(6) group according to the classifications of the collective model, where the typical value is 2.5. The actual values for the nuclei under investigation were (2.66, 2.59, 2.49), but the theoretically estimated values were 2.84, 2.73, 2.57 for the isotopes ${}^{144}_{88}Ba_{56}$,${}^{146}_{88}Ce_{58}$,${}^{148}_{88}Nd_{60}$. correspondingly. The diminished transition probability for electric quadrupole and magnetic dipole transitions, together with the electric dipole moment and effective charge for each isotope examined in this work, were also computed. The mixing ratio E_{41}/E_{21} was computed to ascertain the dominating transition. Upon comparing the theoretical results with the available empirical data, a good concordance was observed, indicating an acceptable level of agreement.

Keywords: IBM-2, medium nuclei, reduced electric quadrupole, reduced magnetic dipole, mixing ratio, Energy levels of nuclei.

1. INTRODUCTION

The amount of spectroscopic data accessible for neutron-rich nuclei, like the ones studied here, has increased dramatically in the last few years [1-4]. These findings present an opportunity for theorists in nuclear physics to enhance and revise current models for a thorough comprehension of nuclear structure [5,6]. The Interacting Boson Model (IBM) has proven to be a valuable method for an extended duration in characterising lowlying nuclear collective motion across diverse mass regions [7-10]. Arim and Ichello's original IBM version was successful in characterising the collective properties of many medium and heavy nuclei [11-13]. The IBM-2 version differentiates between the wave functions of proton and neutron bosons [14]. Following this, IBM-3 and IBM-4 are introduced. In the IBM-1 and IBM-2 models, bosons are classified as pairs of identical nucleons with angular momentum $L = 0$, referred to as s bosons, and $L = 2$, referred to as d bosons. In the IBM-3, there exists a third category of bosons, referred to as bosons, characterised by their composition of distinct types of particles [15-17]. In the IBM-4, there exists an additional boson with $L = 4$, referred to as g-bosons [18]. The latter two forms are confined to a certain area of nucleus. This study will use the IBM-2 version to compute several nuclear characteristics of neutron-rich isotones. ${}^{144}_{88}Ba_{56}$,${}^{146}_{88}Ce_{58}$,${}^{148}_{88}Nd_{60}$.

2. Model theoretical foundation

In IBM-2, the energy levels and gamma transition matrix elements are computed using the Hamiltonian

operator, which is composed of three parts: one for proton bosons, one for neutron bosons, and a third that describes the interaction between different bosons [19].

$$H = H_\pi + H_\nu + H_{\pi\nu} \quad (1)$$

A common form for the Hamiltonian in phenomenological computations is

$$\hat{H} = \varepsilon_d(\hat{n}_{d\pi} + \hat{n}_{d\nu}) + \kappa(\hat{Q}_\pi . \hat{Q}_\nu) + \sum_{\rho=\pi,\nu} \hat{V}_{\rho\rho} + \hat{M}_{\pi\nu}(\xi_1, \xi_2, \xi_3) \quad (2)$$

where the indentation represents the scalar product. The first statement represents the energies of neutrons and protons as single bosons, ε_d, the difference in energy between s- and d-bosons, and n_ρ, the number of d-bosons, where ρ is either a proton or a neutron boson. The quadrupole-quadrupole interaction between neutron and proton bosons of strength κ is the primary component of the boson-boson interaction, which is represented by the second term [20]. We define the quadrupole operator as

$$Q_\rho = \left[d_\rho^+ s_\rho + s_\rho^+ d_\rho^{\sim}\right]^2 + \chi_\rho \left[d_\rho^+ d_\rho^{\sim}\right]^2 \quad \rho = \nu \text{ or } \pi \quad (3)$$

Where $\chi_\rho$defines the configuration of the quadrupole operator and is established experimentally. The square bracket in eq (3) signifies angular momentum coupling [21]. The variables $V_{\pi\pi}$ and $V_{\nu\nu}$ in eq (2), which pertain to interactions among like-bosons, are sometimes used to enhance the alignment with experimental energy spectra. They possess the following structure.

$$V_{\rho\rho} = \frac{1}{2}\sum_{L=0,2,4} C_L{}^\rho \left([d^+{}_\rho d^+{}_\rho]^{(L)} . [d_\rho d_\rho]^{(L)}\right)$$

Nevertheless, their impacts are often seen as insignificant and frequently overlooked. The Majorana term $M_{\nu\pi}$, including three factors ξ_1, ξ_2 and ξ_3, may be expressed as [22]:

$$M_{\nu\pi} = \frac{1}{2}\xi_2([s_\nu{}^+ d_\pi{}^+ - d_\nu{}^+ s_\pi{}^+]^{(2)} . [s_\nu d_\pi - d_\nu s_\pi]^{(2)}) - \sum_{k=1,3} \xi_k([d_\nu{}^+ d_\pi{}^+]^{(k)} . [d_\nu\, d_\pi]^{(k)}) \quad (5)$$

3. Discussion of results and calculations

The isotones used for this study are A=144, 146, and 148, according to the availability of experimental data. Numerous researchers have examined the energy spectrum and electromagnetic characteristics of nuclei in this area using various theoretical simulations [23-26]. The nuclei examined in this research paper are classified as isobars, with a fixed neutron count of N = 88, where the nearest closed shell is 82. Consequently, the number of neutron bosons is constant at N_ν = 3 for all isotopes, while the number of proton bosons is N_π = 3, 4, and 5 for the isobars ${}^{144}_{88}Ba_{56}$, ${}^{146}_{88}Ce_{58}$, and ${}^{148}_{88}Nd_{60}$, respectively. The Hamiltonian parameters in Eq 2 were designated as free parameters to enable their manipulation in order to get optimal theoretical values that closely align with the experimental data. Table 1 presents the parameters used in this study, indicating that some were constant while others were varied, as the values of the boson energy parameter fluctuated between 0.5 and 0.78 MeV in response to the rise in the number of proton bosons. The Maggiore limit was established with $\xi_1 = \xi_3, \xi_2$, since this parameter significantly influences the energy level (2_3), which is characterized by mixed symmetry. These isotopes are classified under the soft gamma O (6) framework, as per the first boson model IBM-1 assessments, situated at an edge of the Casten triangle, where the E_{41}/E_{21} ratio was used to ascertain the nuclei's position on the Casten triangle [27-29]. Following the modification of the parameters, the energy spectrum of the isobars Ba, Ce, and Nd was produced, as illustrated in figures 1, 2, and 3. These figures depict a comparison between the theoretically calculated and experimental values, with the energy levels categorized into ground bands in Figure 1, demonstrating a strong concordance between the empirical and theoretical values, as well as the beta and gamma bands in figures 2 and 3. We observe a moderately acceptable correlation between theoretical and empirical values; however, certain energy levels, specifically 8_1 and

10_1, remain unpredicted by the model, potentially due to extreme rotational states. Consequently, the emphasis was placed on the ground band, focusing on levels 2_1 to 10_1 across all isotopes. The beta band exhibits a significant divergence from the expected values starting at 4_2. Regarding the gamma band for energy levels, we achieved an identical configuration of energy levels, indicating that the model successfully generated the energy spectrum of the gamma band has a similar overall pattern as seen in figure 3. Table 2 presents a comparison of the experimental and theoretical values of the E_{41}/E_{21}ratio. Table 3 presents the experimental data and the IBM-2 estimated values for the energy levels of all isotopes [30].

Table- 1: Parameter values used to generate the energy spectrum in MeV in IBM-2

Nucleus	N_π	N_ν	N	ε	κ	χ_π	χ_ν	$C_{0,2,4}$	$\xi_1 = \xi_3, \xi_2$
$^{144}_{88}Ba_{56}$	3	3	6	0.500	-0.142	-1.2	-0.62	0.16,0.16,0.0	0.015, -0.099
$^{146}_{88}Ce_{58}$	4	3	7	0.660	-0.142	-1.2	-0.62	0.15,0.15,0.0	0.04, -0.040
$^{148}_{88}Nd_{60}$	5	3	8	0.780	-0.143	-1.2	-0.62	0.18,0.18,0.0	-0.080,0.045

Table- 2: Comparison between experimental and theoretical values of the ratio $E_{41}/E_{21}$and E_{61}/E_{21}

Nucleus	calculations	E_{41}/E_{21}	E_{61}/E_{21}
$^{144}_{88}Ba_{56}$	Exp	2.66	4.82
	IBM-2	2.95	5.79
$^{146}_{88}Ce_{58}$	Exp	2.59	5.04
	IBM-2	2.87	5.5
$^{148}_{88}Nd_{60}$	Exp	2.49	4.25
	IBM-2	2.60	4.76

Table- 3: Comparison of the values computed by the IBM-2 model with the experimental values in MeV obtained from the reference [30].

	$^{144}_{88}Ba_{56}$		$^{146}_{88}Ce_{58}$		$^{148}_{88}Nd_{60}$	
J^+	IBM-2	Exp	IBM-2	Exp	IBM-2	Exp
2_1	0.206	0. 199	0.252	0.258	0.302	0.302
4_1	0.588	0.530	0.690	0.668	0.778	0.753
6_1	1.134	0.962	1.297	1.171	1.389	1.280
8_1	1.847	1.471	2.064	1.737	2.110	1.857
10_1	2.707	2.044	2.993	2.352	2.947	2.472
0_2	0.998	1.020	1.091	1.043	1.143	0.917
2_2	1.117	1.315	1.260	1.274	0.918	1.170
4_2	1.524	-------	1.844	1.627	1.282	1.604
6_2	1.992	-------	2.450	1.956	1.872	2.099
0_3	1.659	-------	2.092	1.658	1.556	1.432
3_1	1.612	-------	1.871	1.577	1.208	1.511
2_3	1.356	1.848	1.660	1.382	1.332	1.2489

4_3	1.735	-------	2.057	1.712	1.868	1.683
6_3	2.400	-------	2.741	2.257	2.286	2.149

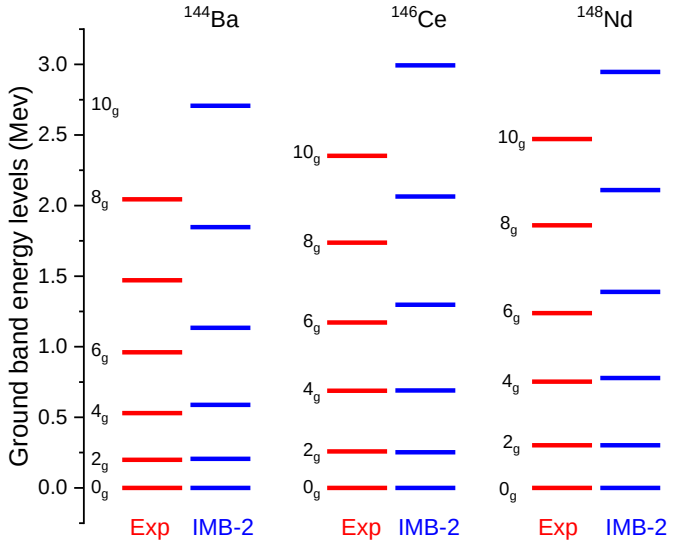

Fig-1: Comparison between experimental and calculated values using IBM-2 bands ground energy levels

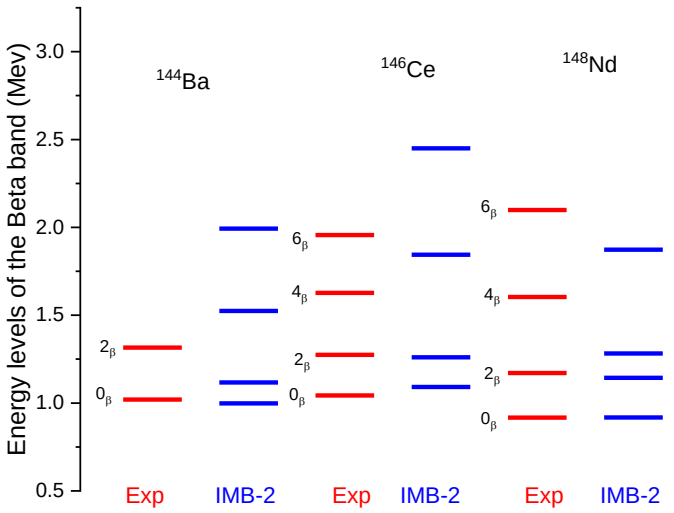

Fig-2: Comparison between experimental and calculated values using IBM-2 bands beta energy levels

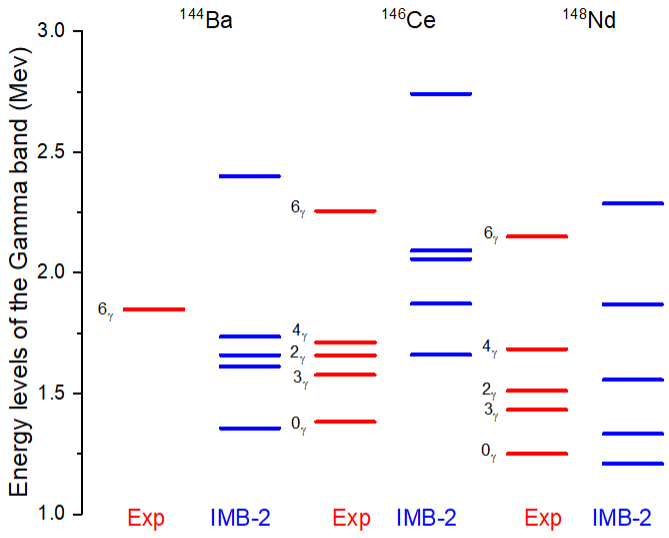

Fig-3: Comparison between experimental and calculated values using IBM-2 bands gamma energy levels

4. Electromagnetic properties

4.1 Reduced electric quadrupole transition probability $B(E2)$

The wave function that is obtained from the diagonalisation of H is used in order to calculate the reduced electric quadrupole transition probability and the quadrupole moment of the 2^+ state. This is done in order to get an understanding of how the IBM-2 Hamiltonian reflects the many physical features of the nuclear system. The following is the definition of the transition operator $E2$ with regard to IBM-2[31]:

$$T^{(E2)} = e_\pi Q_\pi + e_\nu Q_\nu \quad (6)$$

In this context, $Q_\rho$corresponds to the value in eq (3), while e_π and e_ν represent the effective charges of the bosons, which are contingent upon the boson number N_ρ and may assume any value to align with the experimental outcomes. The process for assessing the effective charge value is detailed in reference [32]. The effective charges calculated using this method for the three isotones are shown in Table 4. The computation results are shown in Table 5. The table unequivocally illustrates a robust correlation between the experimental data and the computed outcomes. We have identified discrepancies in certain values. The quadrupole moments of 2_1^+ have been calculated, and the corresponding values are presented in Table 6. There is a single piece of experimental data available. Using the experimental value of $(B(E2); 2_1 - 0_1)$, the quadrupole moment can be calculated through the established relation [33];

$$B(E2; 2 \to 0) = \frac{5}{16\pi} Q_\circ^2$$

$$Q(2_1^+) = -\frac{2}{7} Q_\circ \quad (7)$$

Where $Q_\circ$ represents the static quadrupole moment. Although the connections pertain to collectively deformed nuclei, the substantial significance of the quadrupole moment warrants their use. The projected values consistently exceed one and have a negative sign relative to the experimental value.

4.2 Reduced magnetic dipole transition probability B(M1) and mixing ratio δ(E2/M1)

In the event when I =1, the following is the generic formula for the single boson magnetic transfer operator:

$$T^{(M1)} = \left[\frac{3}{4\pi}\right]^{1/2}(g_\pi L_\pi{}^{(1)} + g_\nu L_\nu{}^{(1)}) \quad 8$$

where g_π, g represent the boson g-factors in units of μN and $L^{(1)} = \sqrt{10}(d^+ x \tilde{d})^{(1)}$. This operator may be expressed as:

$$T^{(M1)} = \left[\frac{3}{4\pi}\right]^{1/2}\left[{}^1/_2\,(g_\pi + g_\nu)(L_\pi{}^{(1)} + L_\nu{}^{(1)}) + {}^1/_2\,(g_\pi - g_\nu)(L_\pi{}^{(1)} - L_\nu{}^{(1)})\right] \quad 9$$

Because the first term on the right side of the eq is diagonal, we may rewrite the preceding eq as for $M1$ transitions:

$$T^{(M1)} = 0.77\left[d^+\tilde{d}\right)_\pi{}^{(1)} - (d^+\tilde{d})_\nu{}^{(1)}](g_\pi - g_\nu) \quad 10$$

Since the components of the $B(M1)$ matrix is often difficult to measure directly, the multipole mixing ratio may be used to represent the $M1$ strength of the gamma transition, as shown in [32].

$$\delta({}^{E2}/_{M1}) = 0.835E_\gamma(MeV).\Delta \text{ where } \Delta = \frac{\langle I_f||T^{E2}||I_i\rangle}{\langle I_f||T^{M1}||I_i\rangle} ineb/\mu N \quad 11$$

After fitting the E2 matrix components, they may be used to get the M1 matrix elements and then calculate the mixing ratio $\delta({}^{E2}/_{M1})$. The g_π and g_ν in eq (10) must be approximated if they have not been measured. The g factors may be estimated from the experimental magnetic moments μ of the 2_1^+ state $\mu = 2g_{total}$ and $\mu = 0.64(8)$. The overall gyromagnetic ratio is documented by Sambataro et al. [34] as follows;

$$g = g_\pi \frac{N_\pi}{N_\pi + N_\nu} + g_\nu \frac{N_\nu}{N_\pi + N_\nu} \quad 12$$

Numerous relations may be derived for a specific mass area, subsequently allowing for the calculation of average values g_π and g_ν for that region. One experimental $B(M1)$ measurement and the previously indicated connection were used to ascertain that $g_\pi - g_\nu = 0.017\mu N$. It is important to recognise that the traditional values of the g factor must conform to the equation $g_\pi + g_\nu = 1\mu N$. The projected parameter values are $g_\pi = 0.33\mu N and g_\nu = 0.31\mu N$; they were used to compute the ratio $\Delta(E2\backslash M1)$ and subsequently the mixing ratio $\delta(E2\backslash M1)$[35]. The ratios for certain transitions in ^{184}Nd were computed, since experimental data for comparison is available; the results are shown in Table 6.

Table- 4: Computed values of the effective charge for each boson, proton, and neutron.

Isotones	$e_\pi efm^2$	$e_\nu efm^2$
$^{144}_{88}Ba_{56}$	0.041	0.215
$^{146}_{88}Ce_{58}$	0.158	0.355
$^{148}_{88}Nd_{60}$	0.100	0.566

Table- 5: Theoretical and experimental values of the transition probability of the reduced electric quadrupole B(E2) in unit e^2b^2

Transition	$^{144}_{88}Ba_{56}$		$^{146}_{88}Ce_{58}$		$^{148}_{88}Nd_{60}$	
	Exp.	IBM-2	Exp.	IBM-2	Exp.	IBM-2
$2_1 \rightarrow 0_1$	0.208(6)	0.203	0.93(13)	0.94	1.37(2)	1.431
$2_2 \rightarrow 0_1$		0.007		0.025	0.075(5)	0.133

$2_2 \rightarrow 2_1$		0.037		0.165	0.085(5)	0.022
$2_3 \rightarrow 0_1$		0.002		0.002	0.073(3)	0.025
$2_3 \rightarrow 2_1$		0.001		0.006	0.026(1)	0.022
$4_1 \rightarrow 2_1$	0.407(61)	0.501		2.628	1.44(6)	2.074
$3_1 \rightarrow 2_1$		0.0161		0.047		0.034
$3_1 \rightarrow 1_1$		0.0196		0.000		0.602
$0_2 \rightarrow 2_1$		0.017		1.288	0.005(1)	0.023

Table- 6: Experimental and theoretical values of electric quadrupole moment in unit fm^2.

Isotones	$[Qfm^2]_{exp.}$	$[Qfm^2]_{theor.}$
$^{144}_{88}Ba_{56}$	-0.68(2)	-1.78
$^{146}_{88}Ce_{58}$	-1.37(19)	-1.54
$^{148}_{88}Nd_{60}$	-1.46(13)	-2.18

Table-7: Theoretical and experimental determinations of the isotope mixing ratio $^{148}_{88}Nd_{60}$

Isotones	Transition energy (MeV)	$I_f \rightarrow I_i$	$[\delta(^{E2}/_{M1})]_{exp.}$	$[\delta(^{E2}/_{M1})]_{theor.}$
$^{148}_{88}Nd_{60}$	0.869	$2_2 \rightarrow 2_1$	+8(+12-2)	+6.92
	0.947	$2_3 \rightarrow 2_1$	-	-0.34
	1.209	$3_1 \rightarrow 2_1$	0.20(4)	-5.12
	0.759	$3_1 \rightarrow 4_1$	+5(+15-22)	-12.1
	0.976	$3_2 \rightarrow 4_1$	0.0(+13-1)	-0.25
	1.427	$3_2 \rightarrow 2_1$	+0.37(5)	+60

References

1. Fioretto, E., et al. "Study of the population of neutron-rich heavy nuclei in the A~ 200 mass region via multinucleon transfer reactions." *EPJ Web of Conferences*. Vol. 163. EDP Sciences, 2017.
2. Bianco, Davide, et al. "Systematic spectroscopic study of neutron rich nuclei within a new shell model context." Journal of Physics: Conference Series. Vol. 533. No. 1. IOP Publishing, 2014.
3. Watanabe, Yutaka, et al. "Spectroscopy of neutron-rich nuclei produced by multinucleon transfer reactions at KISS." EPJ Web of Conferences. Vol. 306. EDP Sciences, 2024.
4. Arthuis, Pierre, K. Hebeler, and A. Schwenk. "Neutron-rich nuclei and neutron skins from chiral low-resolution interactions." arXiv preprint arXiv:2401.06675 (2024).
5. Agodi, Clementina, et al. "Nuclear physics midterm plan at LNS." *The European Physical Journal Plus* 138.11 (2023): 1038.
6. Acosta, Luis, et al. "XLIV Symposium on Nuclear Physics, January 9-12th 2023."
7. Karampagia, sofia g. "approximate dynamical symmetries in collective models of nuclear struture." (2014).
8. Nomura, Kosuke, Noritaka Shimizu, and Takaharu Otsuka. "Formulating the interacting boson model by mean-field methods." *Physical Review C—Nuclear Physics* 81.4 (2010): 044307.
9. Frauendorf, S. "The low-energy quadrupole mode of nuclei." *International Journal of Modern Physics E* 24.09 (2015): 1541001.

10. Macek, Michal. "Classical Chaos in Collective Nuclear Models."
11. Arima, A., and F. Iachello. "Collective nuclear states as representations of a SU (6) group." *Physical Review Letters* 35.16 (1975): 1069.
12. Arima, A., et al. "Collective nuclear states as symmetric couplings of proton and neutron excitations." *Physics Letters B* 66.3 (1977): 205-208.
13. Arima, A., and F. Iachello. "Interacting boson model of collective nuclear states." *Ann. Phys. (NY)* 201 (1978).
14. Nomura, Kosuke. "Low-energy structure and β-decay properties of neutron-rich nuclei in the region of a shape phase transition." *Physical Review C* 109.3 (2024): 034319.
15. Kota, V. K. B. "SU (3) in Interacting Boson Models." *SU (3) Symmetry in Atomic Nuclei*. Singapore: Springer Singapore, 2020. 123-153.
16. Isacker, P. Van. "Algebraic Models of Nuclei." *Handbook of Nuclear Physics*. Singapore: Springer Nature Singapore, 2022. 1-35.
17. Van Isacker, P. "The interacting boson model with SU (3) charge symmetry and its application to even--even N $\approx $ Z nuclei." *arXiv preprint nucl-th/9811014* (1998).
18. Van Isacker, P., et al. "The fermion SO (8) model and its connection with an IBM-4 with L= 0 bosons." *Journal of Physics G: Nuclear and Particle Physics* 24.7 (1998): 1261.
19. Hu, Bao-Yue, et al. "Quadrupole and octupole states in 152Sm using the proton–neutron interacting boson model." *Journal of Physics G: Nuclear and Particle Physics* 50.2 (2023): 025107.
20. Sabbar, Ali N., and Saad N. Abood. "Nuclear Structure of Ce Nuclei within Interacting Boson Model-2." *Asian Journal of Research and Reviews in Physics* 5.3 (2021): 26-33.
21. Nomura, Kosuke. "Two-neutrino double-β decay in the mapped interacting boson model." *Physical Review C* 105.4 (2022): 044301.
22. Al-Sadi, Mohammed Abdul Kadhim Hadi, Qasim Shakir Kadhim, and Salwan Hassan Abdul Zahrah Yasi. "Mixed symmetry states for 70Zn, 72Ge, 74Se, 76Kr isotones by using IBM-2." *Journal of Physics: Conference Series*. Vol. 1234. No. 1. IOP Publishing, 2019.
23. Hamilton, W. D., A. Irbäck, and J. P. Elliott. "Mixed-Symmetry Interacting-Boson-Model States in the Nuclei Ba 140, Ce 142, and Nd 144 with N= 84." *Physical Review Letters* 53.26 (1984): 2469.
24. Chuu, D. S., et al. "Structures of N= 88 and N= 90 isotones in the interacting boson approximation." *Physical Review C* 30.4 (1984): 1300.
25. Zhu, S. J., et al. "Octupole deformation in 142,143 Ba and 144Ce: New band structures in neutron-rich Ba-isotopes." *Physics Letters B* 357.3 (1995): 273-280.
26. Rodríguez, Tomás R., and J. Luis Egido. "A beyond mean field analysis of the shape transition in the Neodymium isotopes." *Physics Letters B* 663.1-2 (2008): 49-54.
27. Casten, R. F. "Simplicity and complexity in nuclear structure." *Romanian Reports in Physics* 57.4 (2005): 515.
28. Van Isacker, P., A. Bouldjedri, and S. Zerguine. "Phase transitions in the sdg interacting boson model." *Nuclear Physics A* 836.3-4 (2010): 225-241.
29. Casten, Richard F., and David D. Warner. "Empirical Tests of the IBM-1." *Algebraic Approaches to Nuclear Structure*. CRC Press, 2020. 129-194.
30. ENSDF, http:// www.nndc.bnl.gov/ensdf (Nuclear data sheet)
31. Jalili-Majarshin, A., M. A. Jafarizadeh, and N. Fouladi. "Algebraic solutions for two-level pairing model in IBM-2 and IVBM." The European Physical Journal Plus 131.9 (2016): 337.

32. Subber, A. R. H., et al. "The level structure of 76Se and 78Se and the systematics of selenium isotopes within the framework of the DDM." Journal of Physics G: Nuclear Physics 13.6 (1987): 807.
33. Robinson, Shadow Jason Quinn, et al. "Shell-model test of the rotational-model relation between static quadrupole moments $Q\ (2_1^+)$, B (E 2)'s, and orbital M 1 transitions." Physical Review C-Nuclear Physics 73.3 (2006): 037306.
34. Sambataro, M., et al. "On magnetic dipole properties in the neutron-proton IBA model." *Nuclear Physics A* 423.2 (1984): 333-349.
35. Navratil, P., B. R. Barrett, and J. Dobeš. "M1 properties of tungsten isotopes in the interacting boson model-2." *Physical Review C* 53.6 (1996): 2794.